UDC 519.652
DOI: 10.20535/SRIT.2308-8893.2024.3.07

FAIRNESS OF 2D COROTATIONAL BEAM SPLINE AS COMPARED WITH GEOMETRICALLY NONLINEAR ELASTIC BEAM

I. ORYNYAK, P. YABLONSKYI, D. KOLTSOV, O. CHERTOV, R. MAZURYK

Abstract. The goal of this paper is to further investigate the properties and advantages of corotational beam spline, CBS, as suggested recently. Emphasis is placed on the relatively simple task of drawing the spline between two endpoints with prescribed tangents. In the capacity of "goodness" of spline, the well-known notion of "fairness" is chosen, which presents itself as the integral from the squared curvature of spline over its length and originates from the elastic beam theory as the minimum of energy of deformation. The comparison is performed with possible variants of the cubic Bezier curve, BC, and geometrically nonlinear beam, GNB, with varying lengths. It was shown that CBS was much more effective than BC, where any attempt to provide better fairness of BC by varying the distances from endpoints to two intermediate points generally leads to lower fairness results than CBS. On the other hand, GNB, or in other words, the elastica curve, can give slightly better values of fairness for optimal lengths of the inserted beam. It can be explained by the more sophisticated scientific background of GNB, which employs 6 degrees of freedom in each section, compared with CBS, which operates only by 4 DoF.

Keywords: corotational beam spline, geometrically nonlinear beam, 2D, Bezier curve, fairness, transfer matrix method.

INTRODUCTION

In this paper we analyze the aesthetical quality, or in other words the fairness of the newly proposed Corotational Beam Spline, CBS [1]. For a few examples, we will also compare the CBS results with those obtained by an accurate Geometrically Nonlinear Beam, GNB, approach [2]. It is done intentionally because sometimes there is confusion as to the difference between the real beam and the beam splines. For the case of small displacements, both approaches are the same – we mean cases of explicit presentation $y = y(x)$, where for example, y is the vertical coordinate of the point, and x is the horizontal one. Yet in the case of large displacements GNB operates by 6 parameters and presents itself as the solution of the differential equation of the 6^{th} order, whereas the explicit beam spline is always the solution of the 4^{th} order equation.

Historically, the beams have generated splines both as technical tools initially, and later as the mathematical model [3]. For many years, starting from early AD Roman times the elastic beams (long and thin strips of wood) have been used by draftsmen to fair in a smooth curve between specified points for shipbuilding [4]. Mathematical cubic spline approximation in its present form was suggested in 1957 by Holladay [5]. He noted that for curves with modest slopes,

the cubic spline became identical to the bending of a straight beam. The latter operates by four degrees of freedom – displacement, angle of rotation (first derivative), bending moment (second one), and transverse force (third one). To apply the beam spline the positions of consecutive points should be known and one additional boundary condition should be specified at each end. The beam spine is called the natural one if the second derivative is taken as zero. In beam theory, this corresponds to simply supported end, when displacement is fixed, and moment is zero.

The language and technique of the beam theory were fruitfully employed later. Mention only a few ideas. First of all, in analogy to beam the different end conditions can be considered [3; 6]. They are: free end conditions, when second and third derivatives (moment and force) are equal to zero and the position is unknown; the clamped one, when the position and angle (first derivative) are prescribed; zero force condition (third derivative is additionally equal to zero). Another finding of the beam theory is the employment of the tensed beam model to use in beam spline – this is to make the spline straighter [7] at the expense of increased curvature at the prescribed positions (control points). Instead of the 3rd-order polynomial the 1st-order polynomial and two exponential functions, $\exp(\pm kx)$, are used, where coefficient k is proportional to the square root of the prescribed axial force (used in addition to the usual transversal one) [8]. Note, that if $k \to 0$ we get the usual beam spline. Also note, that 4 parameters tensed beam model is a simplification of 6 parameters planar beam problem (analog of the elastica).

Mention some additional beam features suggested during the "golden age" of the beam domination in the spline development. Very effective is the application of the beam on the elastic support model instead of the usual rigid ones, where the curve was suspended by springs attached to its control points for smoothing the errors of measurements [9]. The spring stiffness controls how closely the beam interpolates these points [10]. Asker [11] introduces several approaches to overcome wiggles [12]. The variable beam stiffness is in a piecewise constant fashion and in a piecewise linear fashion, which allows to change locally the spline behavior while keeping the same control points. As noted in [12] these methods are equivalent to the weighted spline of Salkauskas [13].

The main drawback of 'classical' beam splines is that they are suitable only for interpolation to plane curves, which turn through an angle of less than 180° [14]. The reason is the explicit presentation of the form $y = f(x)$, which is axis dependent and is not able to represent multiple-valued functions, and cannot be used where a constraint involves an infinite derivative [15].

So, generally, for any geometry, the implicit representations of the form $f(x, y) = 0$, and parametrical representation of the form $y = f(t)$ and $x = g(t)$, where t is an additional parameter, are used for curve splines [15]. As to beam splines in particular, Ferguson [16] introduces the parametric cubic spline curve by applying the cubic spline function for each coordinate by employing the independent curve parameter t, by prescribing for each consequent vector point (x, y) the non-decreasing value of parameter t. Their drawback is in the arbitrariness of the parameter t, the choice of which leads to different configurations [17], especially in smoothing the sharp corners [18], or in general, in case of large curvature [19]. Of course, it can be 'repaired' by imposing the additional re-

quirement to transverse force (third derivative), by changing the positions of corner points [18], but it implies additional complications. So, the parametric beam spline is rarely used nowadays.

Very popular now are splines based on Bezier curves, B-splines, and NURBS [15]. Their peculiarities are that they are formed by special polynomial or rational functions, and the sum of them in each control point is equal to 1. Other kinds of curves are used very often, too [19; 20]. Nevertheless, despite of present less usability, the cubic beam splines have tremendous historical significance and a large impact on the development of the spline theory. We can formulate, at least, three of their salient contributions.

1. The quantitative notion of the curve aesthetic measure or 'fairness'. The number of curves passing through a set of points is infinite, thus the interpolation problem is by nature ill-posed [21]. So convenient criteria for the best curve must be formulated. Of course, the notion of a fair curve appeared long before the origin of cubic beam spline, and various qualitative formulations were abundantly employed in literature [12; 21]. However, the first mathematically exact definition was based on the analogy with the elastic beam theory, where the energy of deformation E is given by expression [5; 8]:

$$E = \int_0^L \kappa^2(l)dl \,, \tag{1}$$

where κ is the curvature, l is an element of length, and L is the length. So, the curve is deemed to be the best, if it provides the minimum of energy E. In the context of CAD, this integral becomes one of the standard criteria for the fairness of a planar spline curve [22]. Note, that cubic splines give the minimum energy only in case of small deflections.

The expression (1) for the energy E very often is supplemented by other components, which also have the 'beam' origin. For example, for a 3D beam, it is common to introduce the 'stretch' energy, which is proportional to the 'elongation' of the beam and is the integral from the squared first derivative, or the 'twist' energy, which is found as the integral from the squared third derivative (rotation of the beam) [23]. For approximation spline, the control points are often considered as the springs [10], and the extension or compression of which makes the additional contribution to the elastic energy. So, an additional term for each "spring' (control) point is considered, which is proportional to the squared difference between the position of the spring and smoothened points [24]. Such curves are named minimal energy curves, MEC, [12].

Of course, the beam-based energy criteria are not unique mathematical formulations for defining the best curve. Other formulations are widely used, too, but they were either inspired by the energy criteria analogy or emerged as a result of the drawback of MEC for the best curve construction. Explain this. When the length of the spline is not restricted, the best MEC (mathematically) may be attained for the spline of infinite length and minimal curvature [25].

So, in general, MEC does not correspond to the common requirement of Farin [26], that a curve's curvature plot must be almost piecewise linear, continuous, and with only a small number of segments. So, a different functional, which satisfies Farin's criteria, the so-called minimum variation curve, MVC, was proposed in [12]. Instead of $\kappa^2(l)$ in functional (1) the square of the derivative of

curvature $\left(\frac{d\kappa(l)}{dl}\right)^2$ is used. In contrast to the MEC which bends as *little* as possible, the MVC bends as uniformly or as smoothly as possible [12]. Yet the MVC has no clear physical sense, it is not as flexible as the MEC to account for other constraints, for example, for the required proximity to the control points at approximation.

So, the MEC are still widely used in the usual continuous [22] or discrete form [27], where the energy is accounted for integrally in the control points as the sum of squared angular misalignments. The minimization of functional can give an aesthetically pleasant curve, which is stable for relatively slowly changing angles between neighboring control points. Very often the energy minimization is applied as a polishing tool for curves, which are derived by other kinds of splines. For example, in many works, energy minimization is applied to Bezier curves [28; 29], cubic spline curves [30], biarck splines [31], B-splines [32], for Hermite splines [33], and many others.

2. Development of the technique of construction of *elastica* and promotion of its popularity. The notion of elastica originated at the end of the 17th century due to the efforts of the Bernoulli brothers [34]. The elastica is the free-form deformation of the elastic beam, whose shape is such that its squared curvature (1) was minimized. It was an interesting mathematical task, and many famous scientists contributed to its solution and application to different problems, to mention only Euler, Laplace, Kirchhoff, Max Born, Love, etc [34].

The practical resurrection of interest in elastica originated in the works of Schoenberg [34] in 1946, where the spline was defined as a variational problem that minimizes the functional (1) but makes the small-deflection approximation. The basic shortcoming of the works of Schoenberg and Holliday [34] was underlined by Birkhoff and de Boor in 1965 [35], where it was noted that linearized interpolation schemes are not invariant under rigid rotation. So, they suggested replacing linearized spline curves with non-linear splines (or "elastica"). Furthermore, they obtained the differential equation for curvature functions $\kappa(l)$, which satisfy to minimum energy requirement (1):

$$\ddot{\kappa}(l) + \frac{1}{2}\kappa^3 = 0 . \qquad (2)$$

This curve was treated as a free elastic curve as it refers to a planar elastic curve without length constraints. This result was extended in work [36], where it was shown that equation (2) can be applied for segmented curvature function with natural end conditions that pass through a prescribed set of control points. Other generalization of these results consists in the justification of the validity of equation (2) when the end conditions are given in the form of prescribed tangents [37].

Based on these general results the various algorithms of elastica construction were proposed. The first work on the numerical construction of elastica was proposed by Glass in [38], where the discrete points on the curve were specified iteratively. Technically this algorithm was later improved by Malcolm [39]. Mehlum [40] used circular arc approximation of arbitrary precision. Mehlum uses these methods in the Autokon system for curve and surface design, which became the first commercial CAD software, and underlined the tight relation between

free-form shape representations and physically inspired mathematical functions [41]. Another technique of nonlinear spline construction was suggested in [22], where the looking for function is presented as a piecewise polynomial curvature function.

Among the many early works on nonlinear elastica, we see the work of Horn [42], where it was carefully studied a specific MEC segment, defined by two points on a baseline with a vertical tangent constraint specified at each point. The approach consists of a presentation of the looking-for curve as a set of circular arcs with a minimization of energy. Starting from one arc, then two or more arcs up to sixty-four were considered, while the resulting curve resembles a croquet hoop. The resulting energy was as small as 0.913953% of the semicircle. Then the elliptical curve with minimal energy was constructed and energy was equal to 93.42% of the semicircle, and for the Cornu spiral the energy was as low as 0.9178%. Then Horn computes closed-form expressions for the energy, arc length, and maximum curvature of his subject curve and the lowest value is equal to 0.913893. MEC has at least two principal shortcomings: the first cause it to fail a very desirable property for splines such as roundness [21], and another one, is that energy depends on an unspecified length of elastica. So, in the works of Kallay [43; 44] the theoretical substantiation and numerical method are elaborated for computing that shape, given the positions and directions of the endpoints and the total length. In this case, the notion of energy and the goal of optimization become clearer and are related to the fixed length. In work [45] the elastica is constructed by the elastic curve segments which are expressed in a closed form via the elliptic functions. The method depends on the good initial guess for the approximating curve with subsequent application of gradient-driven optimization.

On the other hand, the analytical solution for Euler's Elastica motivated within the structural mechanical community the development and application of one-dimensional theories for the deformation of elastic slender bodies [46] and especially the elaboration of the comprehensive and efficient numerical formulation [47]. Geometrically nonlinear computational models of the beam under finite rotation are obtained from three basic approaches: total Lagrangian, updated Lagrangian, and Co-rotational [47]. It is beyond the goal of the paper to discern them in detail.

We only mention that technically they often are reduced to solution by the transfer matrix method, TMM, either within the Lagrangian approach [48] or in the corotational formulation [49]. The transfer matrix, which relates the set of governing parameters at any point of the element including its end with those at the beginning of the element, is called the field transfer matrix, FTM. It is derived by the solution of physical differential equations. The continuity relations between the parameters of two neighboring elements at the border between them are given by the point transfer matrix, PTM. Sometimes the method is called in literature as a method of initial parameters [50]. The transfer matrix method is a very effective tool, which allows to eliminate the intermediate unknowns of inner elements, thus while keeping a large number of degrees of freedom, technically it reduces the ultimate matrix to the size determined only by the number of real points [51].

3. Employment of local coordinates system for each element. In structural mechanics, this approach is called a corotational approach [52; 53]. Here, the total

configuration of a beam is presented as the sum of two components: straight elements position and pure deformational displacement of points. The deformation is measured from a rotating frame attached to the straight element, and linearized formulation solutions are employed in the numeric incremental procedure. The nonlinearity is accounted for by the rotation matrix between the elements. So, the discontinuous angles of rotation between elements are the key parameters of the corotational scheme. Note that the geometrically nonlinear beam model of work [2] is the enhanced corotational approach, where the reference geometry is part of a circle and already contains build-in deformation (basic solution), which is supplemented by smoothing solution derived by integration of governing linear differential equations written in curvilinear (polar) coordinates.

Within the computer graphics world, the looking for curves are usually presented as continuous ones at every stage (iteration) of computation. The only known exception is the Fowler–Wilson method [54], which was based on usual cubic beam splines in a local two-dimensional coordinate system. The Fowler-Wilson scheme is a transition from the explicit presentation of spline $y = f(x)$ to the implicit one $g(x, y) = 0$. It was very popular till the beginning of the 21st century and was used in many industries around the world [55]. So, initially, the spline is given by a set of straight sections, which determine the tangent vector and normal vector. Local sections of the spline are calculated along the normal to the section. The main requirement is to provide the continuity of slope and curvature at the borders between points. The nonlinear equations of continuity are obtained and iteratively solved.

Now return to the goal of this paper. The corotational beam spline of our work [1], among other ideas, uses the idea of straight initial sections drawn between control points, which determine the local system of coordinates. So, the purpose of splines is to smooth out the so-called misalignment (gap) angles. This resembles the idea of Fowler–Wilson. As to the task of interpolation, the main differences in our work [1] consist of two peculiarities. First, from the very beginning, our spline is constructed in a linearized statement, which is usual for the theory of beam:

$$\operatorname{tg}\theta \approx \sin\theta \approx \theta\,, \tag{3}$$

where θ is the calculated angle of rotation, this noticeably simplifies the calculations [56; 57]. Second, to suppress the errors induced by (3) we introduce the notion of auxiliary ‘imaginary’ points. So, we consider that control points are of two kinds. Points of the first kind are of the real kind, where the outer constraints are explicitly given. Points of the second kind are imaginary ones, which are arbitrarily placed between the real ones, their positions are not specified and naturally refined during the calculation process. They are intended to: a) make the length of the straight section approximately equal to the length of the spline section; b) decrease the maximal calculated angle θ within each section to provide better accuracy of (3). Another enhancement of the method is of technical significance and consists of the employment of the transfer matrix method, which allows keeping the resulting matrix for spline with imaginary points of the same dimension as without them. Besides, the geometrically exact definition of curvature is used.

The goal of the paper is to analyze the aesthetical quality or energy (1) of the CBS and compare it with GNB for example a simple task defined by two end-

points with a tangent constraint specified at each point. This choice is taken because: 1) similar tasks were considered in old theoretical investigations of elastica [42; 44]; 2) the fairness of such curve can be easily assessed visually; 3) it is a practical task for thin deformable wire held at each end by a robotic gripper [58] and for applications of robotic hot-blade cutting [45; 59].

THEORETICAL FOUNDATION OF CBS AND GNB

Short introduction to CBS

Note, that very simplified logic, designations, and equations of more general paper [60] are outlined here. The main reason for simplification is that here we consider only the task of interpolation, so many enhancements related to consistency with the task of approximation will be omitted. Note, that the solution process is organized according to the transfer matrix method, TMM, methodology.

Let we have enumerated consequently both the exactly measured (real) points and the inserted between them (in any number) imaginary points, $A_m(X_m, Y_m)$, where m is the point number, and X_m, Y_m are their Cartesian coordinates in the absolute coordinate system. Usually, we do not discern between them and name them as the control points, because referring to the transfer matrix method, TMM, the field transfer matrix, FTM, is the same for any element placed between any two neighboring points. The difference exists only for the point transfer matrix, PTM, and depends on whether the considered point is a real or imaginary one. So, in this case, the points will be discerned by using the additional lower indexes: *"r"* for real points, and "*i*" for imaginary ones. For example, $A_{m,r}$ means that point A_m is the real, and $A_{m,i}$ is the imaginary one.

Connect the consequent points A_m by straight lines and get the open or closed polygon. Consider the particular straight beam section, named as m section, which is placed between control points A_{m+1} and A_m, Fig 1. Introduce the notion of iteration number, k. The real points retain the same position at each iteration; however, the imaginary points change their position. Furthermore, the algorithm envisages that new imaginary points might be inserted during the iteration process. This is controlled by the maximal value of calculated angle θ, as to condition (3). If the angle is large enough, say, larger than $\frac{\pi}{30}$, we insert a new imaginary point. This provides the accuracy as to (3) within 0.2%. So, the insertion of a new imaginary point may change the general enumeration. Thus, the numeration is iteration dependent, and control points should be presented as $A_m^k(X_m^k, Y_m^k)$, where k is the iteration number. Nevertheless, in most cases, the upper index k will be omitted.

The vectorial length of each beam section is designated as $\vec{l}_m$:

$$\vec{l}_m = \vec{A}_{m+1} - \vec{A}_m = (X_{m+1} - X_m)\vec{i} + (Y_{m+1} - Y_m)\vec{j}\,. \qquad (4)$$

For each straight section introduce the local coordinate system (s_m, w_m) and basic vectors $\vec{t}_m$ and $\vec{n}_m$. The tangent local vector $\vec{t}_n$, is derived from (4):

$$\vec{t}_m = \frac{\vec{l}_m}{\left|\vec{l}_m\right|} = a_m\vec{i} + b_m\vec{j},$$

where

$$\left|\vec{l}_m\right| = l_m = \sqrt{(X_{m+1} - X_m)^2 + (Y_{m+1} - Y_m)^2}.$$

The normal vector $\vec{n}_m$ is perpendicular to $\vec{t}_m$ and rotated clockwise concerning it, Fig 1. Local coordinate system (s, w) is related to the basic vectors, where s is counted from $\vec{A}_m$ in the direction of $\vec{t}$, and w is directed as $\vec{n}$. Vector $\vec{n}_m$ is presented as:

$$\vec{n}_m = c_m\vec{i} + d_m\vec{j},$$

where

$$\begin{pmatrix} c_m \\ d_m \end{pmatrix} = \begin{pmatrix} \cos(-\pi/2) & -\sin(-\pi/2) \\ \sin(-\pi/2) & \cos(-\pi/2) \end{pmatrix} \begin{pmatrix} a_m \\ b_m \end{pmatrix} = \begin{pmatrix} 0 & 1 \\ -1 & 0 \end{pmatrix} \begin{pmatrix} a_m \\ b_m \end{pmatrix}.$$

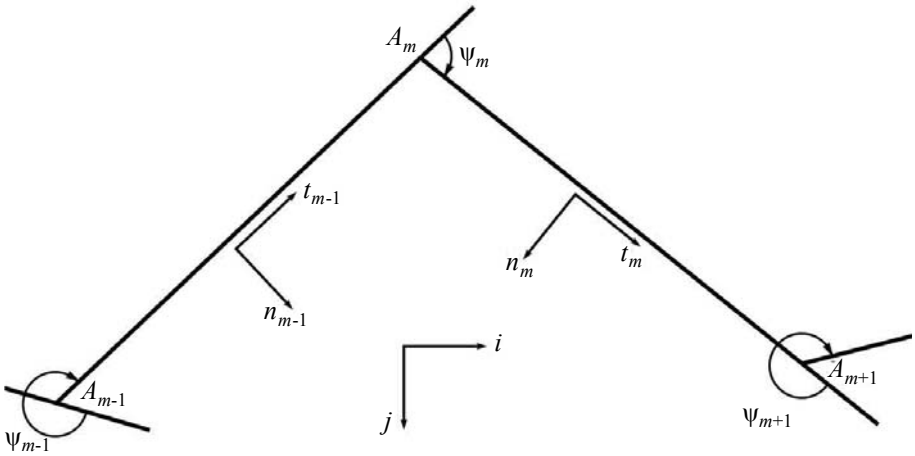

Fig. 1. The global cartesian vectors and local corotational basis for each element

Important in the model is the misalignment angle between two adjacent straight beam sections: m and $m-1$, denoted as ψ_m, Fig. 1. It is counted clockwise from vector $\vec{t}_{m-1}$ to vector $\vec{t}_m$. The angle of misalignment ψ_{m-1} is found from the scalar and vector products of these two vectors:

$$\sin(\psi_m) = \vec{t}_{m-1} * \vec{t}_m, \quad \cos(\psi_m) = \vec{t}_{m-1} \cdot \vec{t}_m. \tag{5}$$

Application of both rules is needed to establish the correct angle quadrant.

Now describe the calculation model. Consider the simplest beam model for an initially straight beam. Each straight beam section is characterized by the vector of state $\vec{Z}(s)$, which is formed by 4 scalar functions of length coordinate s:

$$\vec{Z}(s) = \text{column}\,\{W(s);\ \theta(s);\ M(s);\ Q(s)\},$$

where following the beam traditions we operate by four physical values: $W(s)$ is displacement directed along the local normal vector $\vec{n}$; $\theta(s)$ is the angle of (de-

formational) rotation of the beam axis concerning initial vector $\vec{t}$, directed clockwise; $M(s)$ is the bending moment; $Q(s)$ is the transverse force. The direction of the two latter parameters is chosen so, that the following differential dependencies between all parameters are positive [1]:

$$\frac{dW(s)}{ds} = \theta(s); \quad \frac{d\theta(s)}{ds} = \frac{M(s)}{EI}; \; \frac{dM(s)}{ds} = Q(s); \; \frac{dQ(s)}{ds} = 0, \tag{6}$$

where EI is the constant of the beam, taken below as 1. The solution of the system (6) can be presented in matrix form suitable for the application of TMM:

$$(\vec{Z}_m(s)) = [p_{i,j}(s)](\vec{Z}_{m,0}), \tag{7}$$

where $\vec{Z}_0 = \vec{Z}(s=0)$ is the vector of state in the initial point of the section considered, and the coefficients of the transfer matrix are the following:

$$[p_{l,j}(s)] = \begin{bmatrix} 1 & s & \frac{s^2}{2} & \frac{s^3}{6} \\ 0 & 1 & s & \frac{s^2}{2} \\ 0 & 0 & 1 & s \\ 0 & 0 & 0 & 1 \end{bmatrix}.$$

Note, that equations (7) can give the values of each parameter at the endpoint of each element through the initial parameters at this element by letting $s = l_m$, i.e.:

$$(\vec{Z}_m(l_m)) = (\vec{Z}_{m,1}) = [p_{i,j}(l_m)](\vec{Z}_{m,0}),$$

where lower indexes “0” and “1” mean the beginning and the end of a section, correspondently.

To formulate the calculation scheme, we need to supplement the FTM (7) with PTM equations, which relate the vector of state at the border between the end of the previous and the beginning of the next sections. For real control point, we have the following PTM relations:

$$W_{m,0} = W_{m-1,1}, \tag{8}$$

$$\theta_{m,0} = \theta_{m-1,1} - \psi_m, \tag{9}$$

$$M_{m,0} = M_{m-1,1}, \tag{10}$$

$$Q_{m,0} = Q_{m-1,1} + P_m, \tag{11}$$

$$W_{m,0} = 0. \tag{12}$$

Here P_m is an unknown force in the beam support (real control point). Generally speaking, this force is determined from condition (11), or put more correctly, the introduction of additional unknown P_m requires one additional condition (12). When compiling the system of governing the equation (11) (and unknown P_m) is not used. Condition (8) means that displacement (deviation of

position from the initial straight line) should be the same. Condition (9) is to provide the tangent continuity of the deformed contour, where the deformational angles compensate for the initial misalignment angle. Condition (10) is the equality of approximate beam curvatures. Condition (12) requires that the position of the considered control point should not change during the iteration, i.e., it is fixed.

The point transfer matrix in the case of the imaginary point is slightly different. They require continuity up to 3rd order, i.e., including the transverse force. So, we have:

$$W_{m,0} = W_{m-1,1},$$

$$\theta_{m,0} = \theta_{m-1,1} - \psi_m,$$

$$M_{m,0} = M_{m-1,1},$$

$$Q_{m,0} = Q_{m-1,1}.$$

Or in matrix form

$$(\vec{Z}_{m,0}) = [I](\vec{Z}_{m-1,1}) + \vec{C}_{m,i},$$

where $\vec{C}_i$:

$$\vec{C}_{m,i} = \text{column}\{0; -\psi_m; 0; 0\}.$$

In this case, the PTM does not contain any additional unknowns.

Let's go to the organization of the calculation process by TMM. It is convenient to start with an introduction of four unknown parameters for both the beginning and end of each element. It means we have 8 unknowns for each element. If the number of elements is M, then the number of unknowns is $8 \cdot M$. There are 4 FTM equations for each element, thus at the whole, there are $4 \cdot M$ FTM equations. On the other hand, there are $M-1$ borders between elements for open polygon, for which $4(M-1)$ PTM can be written. So, for an open polygon, $8 \cdot M - 4$ equations should be supplemented by 2+2 boundary conditions on each boundary. One of them is the condition of zero displacement, while another is either the requirement to the angle value, or requirement to curvature (moment), or to transverse force. When the contour (polygon) is closed we have no boundary conditions, but instead, one additional PTM (four conditions) is to be written at the point where the last section meets the first one.

At first glance, accounting for possibly a large number of imaginary points in this CBS technique requires too many unknowns and can be very slow. First, show that imaginary points and related unknowns actually can be removed from consideration. Consider two adjacent sections which are separated by imaginary points. According to the procedure of elimination [51] write three transfer matrixes between them:

$$(\vec{Z}_{m,1}) = [p_{i,j}(l_m)](\vec{Z}_{m,0}), \tag{13}$$

$$(\vec{Z}_{m+1,0}) = [I](\vec{Z}_{m,1}) + \vec{C}_{m,i}, \tag{14}$$

$$(\vec{Z}_{m+1,1}) = [p_{i,j}(l_{m+1})](\vec{Z}_{m+1,0}). \tag{15}$$

Substituting (14) into (15) and later (13) in the resulting equation we formally can get the matrix equation:

$$(\vec{Z}_{m+1,1}) = [p_{i,j}(l_{m+1}, l_m)](\vec{Z}_{m,1}) + \vec{D}_{m,i}, \tag{16}$$

where elements of matrix $p_{i,j}(l_{m+1}, l_m)$, and free terms vector $\vec{D}_{m,i}$ are easily calculated from (13)–(15). The matrix equation (16) is FTM for the combined element, which starts at the point $\vec{A}_m$ and ends at point $\vec{A}_{m+2}$, thus eliminating the imaginary point $\vec{A}_{m+1}$. So, two FTM and one PTM are substituted by one FTM. Second, for the remaining real points the number of unknowns can be reduced to unknown moments in them only, as it is usually given in the textbooks [8].

Note, that calculated values of Mc have dimension of curvature and the meaning of curvature in beam theory formulation. Yet they are not exact geometrical curvatures. So, the additional procedure of refining the values of curvature based on exact differential geometry formulation was established in [1] and will be used in the presentation of the results.

Main equations of GNB

The principal distinction of GNB from spline is that it operates by a real object with real properties and, especially it has a given length, L. In calculations, it is broken into a necessary number of elements. For each element, m, the notions of the Basic, $\vec{B}_m(s)$, and Smoothing, $\vec{S}_m(s)$, solutions are introduced [2; 61], where s is a curvilinear abscissa of any point of element. Then, the looking for Ultimate solution, $\vec{U}^k(s)$, is the sum of these two constituents:

$$\vec{U}^k = \vec{B}^{k-1} + \vec{S}^k. \tag{17}$$

Here the upper index k means the iteration number. So, as follows from presentation (17) the basic solution is a result of the previous iteration $i-1$. Note, that, where possible, the lower and upper indexes m and k will be omitted.

The main aim of the basic solution, BS, is to principally account for all nonlinearities, while the smoothing solution, SS, is a linearized analytical correction to BS. Another purpose of BS is that it gives the system of local curvilinear coordinates and directions concerning which the SS is derived. On the other hand, BS is permanently refined from iteration to iteration as a result of accounting for the present SS. New BS is refined according to the following rule:

$$\vec{B}^k = \vec{B}^{k-1} + g \cdot \vec{S}^k, \tag{18}$$

where g, $0 < g \le 1$ is the so-called retardation coefficient, which restricts the absolute change of BS and accounts for whether the process of solution is convergent (m can be increased) or divergent (m should be decreased). The rule (18) is schematic because not all components of SS are used in BS. For the 2D case, BS geometrically presents itself the part of a perfect circle, the radius of which R_m^k, (or curvature $\kappa_m^k = 1/R_m^k$) and current length l_m^k are related with basic (embedded in) bending moment and axial force [61].

SS solution is formulated for each element in the local curvilinear system of coordinates, Fig. 2. It operates by six governing parameters, as opposed to a

straight beam (cubic spline). They are: two force parameters – transverse force Q and axial force N, bending moment M, angle of rotation θ, and two displacement parameters — normal one w, and tangential one u. These parameters are related by six differential equations:

$$\frac{dQ}{Rd\phi}+\frac{N}{R}=P_n;\ \ \frac{dN}{Rd\phi}-\frac{Q}{R}=P_t;\ \ \frac{dM}{Rd\phi}=Q;$$

$$\frac{d\theta}{Rd\phi}=\frac{M}{EI};\ \ \frac{du}{Rd\phi}-\frac{w}{R}=-\frac{N}{EF};\ \ \frac{dw}{Rd\phi}+\frac{u}{R}=\theta.$$

In the subsequent application below we will not consider the action of outer distributed forces P_n and P_t, and neglect the axial elongation, i.e., take $\frac{1}{EF}=0$.

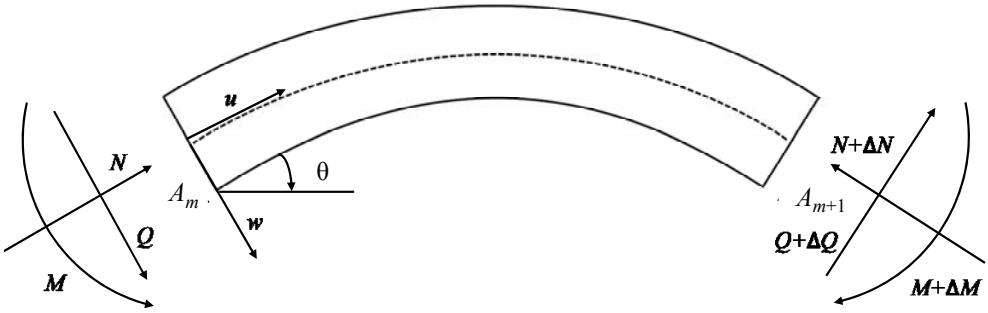

Fig. 2. General scheme of 2D curvilinear beam

The general solution of (5) for SS can be presented in the form suitable for the application of TMM [61], and schematically is given below. For FTM it can be written as [61]:

$$(\vec{Z}_m(s))=[p_{i,j}(s)](\vec{Z}_{m,0}),$$

where elements of matrix $p_{i,j}(s)$ are the solution of the differential equations (5), and the vector of state in any point s is:

$$\vec{Z}(s)=\text{column}\,\{w(s);u(s);\theta(s);M(s);Q(s),N(s)\}.$$

For PTM a similar equation can be written [61]:

$$(\vec{Z}_{m,0})=[H](\vec{Z}_{m-1,1})+\vec{C}_{m,i}.$$

In this case, the matrix $[H]$ is not an identity matrix, due to the vectorial essence of two force and two displacement parameters and different local vectorial basis used. As to the vector of free terms $\vec{C}_{m,i}$, its all components are nonzero due to the discontinuity of the basic solution (so-called gaps [61]). Note that the GNB approach requires three boundary conditions at each end of the beam.

The aim of this short introduction to GNB is twofold. First, to show that the technical solution of GNB can be similarly organized by TMM, with formal elimination of all points (sections) that do not contain the real constraints. Second, the variety of tools and possibilities of GNB analysis by numerical TMM is much richer than in the traditional elastica approach. Hint the few possible

opportunities. If one wants to make the solution "more tensed", it can be very easily done by introducing the normal pressure P_n. To "tense" or to "relax" the particular section it needs to increase or decrease the bending stiffness EI, or to make it variable. The length of particular sections or the beam as a whole can be controlled by axial stiffness EF.

Calculated curvatures in each curved section are presented as the sum of basic curvature (constant) and those induced by calculated bending moment $M_m^k(s)$:

$$\kappa_m^k(s) = \frac{1}{R_m^k} + \frac{M_m^k(s)}{EI}.$$

Four points-based Bezier spline

Consider set of four consequent control points $A_1(X_1,Y_1)$, $A_2(X_2,Y_2)$, $A_3(X_3,Y_3)$, $A_4(X_4,Y_4)$, or in vectorial form:

$$\vec{A}_m = X_m\vec{i} + Y_m\vec{j}; \quad m = 1,2,3,4.$$

They can be used for the construction of a third-order Bezier curve, $\vec{P}(x,y)$ [15]:

$$\vec{P}(x,y) = P_x\vec{i} + P_y\vec{j} = \vec{i}\cdot\sum_{m=1}^{4} X_m\cdot K_m(t) + \vec{j}\cdot\sum_{m=1}^{4} Y_m\cdot K_m(t); \quad 0\le t\le 1,$$

where $K_m(t)$ are the Bernstein's functions

$$K_1(t) = (1-t)^3, \quad K_2(t)(t) = 3t(1-t)^2, \quad K_3(t) = 3t^2(1-t), \quad K_4(t) = t^3.$$

Bezier splines have the following properties [15], important to our task:

1. The first and last points on the curve are coincident with the first and last points of the control polygon.

2. The tangent vectors at the ends of the curve have the same direction as the first and last polygon spans, respectively.

So, our subsequent task is to construct a spline, which starts in point $\vec{B}_1$ at the angle φ_1 with a horizontal axis and ends in point $\vec{B}_2$ directed at angle φ_2. Introduce the unitary tangent vectors $\vec{\eta}_1$ and $\vec{\eta}_2$ in these boundary points. They can be written as:

$$\vec{\eta}_1 = \vec{i}\cdot\cos\varphi_1 + \vec{j}\cdot\sin\varphi_1; \vec{\eta}_2 = \vec{i}\cdot\cos\varphi_2 + \vec{j}\cdot\sin\varphi_2.$$

So, four consequent points of cubic Bezier splines can be chosen as follows:

$$\vec{A}_1 = \vec{B}_1, \quad \vec{A}_4 = \vec{B}_2, \quad \vec{A}_2 - \vec{A}_1 = D_1\cdot\vec{\eta}_1; \quad \vec{A}_4 - \vec{A}_3 = D_2\cdot\vec{\eta}_2,$$

where D_1 is an absolute distance from point $\vec{A}_2$ to point $\vec{A}_1$, and D_2 from $\vec{A}_4$ to point $\vec{A}_3$.

Our next task is to obtain the element of length in each point, $ds(t)$, and the curvature $\kappa(t)$. According to differential geometry rules, we can write:

$$ds = \sqrt{(P_x')^2 + (P_y')^2}\,dt\,, \quad \kappa(t) = \frac{P_x'' P_y' - P_y'' P_x'}{\left(\sqrt{(P_x')^2 + (P_y')^2}\right)^3}\,.$$

These expressions will be used in the calculation of the Brazier spline quality.

EXAMPLES OF CALCULATION

Several similar problems will be calculated and compared here. In some cases, the well-known Bezier curve will be used too. We will consider the relatively simple task, which is defined by two endpoints with a tangent constraint specified at each endpoint.

Example task 1

First point B_1 is placed in point $(X = 0, Y = 0)$, second point B_2 has coordinates $(X = 150, Y = 0)$, the tangent in point B_1 is directed vertically, i.e., the angle (in the clockwise direction) with the horizontal axis is equal $-90°$, and in point B_2 the angle is equal to $90°$. It is the famous Horn task [42], which has demonstrated that minimization of energy is not always a solution for the best curve, and eventually led to the appearance of other criteria, say minimization of squared derivative from curvature [12].

Intuitively, the best curve is the semi-circle of diameter equal to 150. Its length, L_0 is $L_0 = \pi\frac{150}{2} = 235.62$. Calculate the quality (energy) of the ideal semi-circle. According to (1) it is equal to $E_0 = \left(\frac{2}{150}\right)^2 \frac{\pi 150}{2} \approx 0.041888$.

Construct the splines according to different techniques, Fig. 3. Designation BZ 110 relates to the Bezier spline, where two intermediate points on the prescribed tangent are placed at a distance of 110 from either endpoint. Similarly, the BZ 115.5 curve employs one point on distance 115.5 on each tangent. GNB depends on the prescribed length of the beam, so the designation GNB 230 means that the length of the beam is equal to 230. Many variants of BZ spline and GNB can be obtained. As to CBS, it gives only one possible configuration.

Analyze the results. First of all, note that CBS gives the ideal semi-circle. As to other curves, at first glance, they can approach the ideal figure very well, and each seemingly is capable of depicting the ideal circle.

With this respect, the more informative are graphs of curvature versus the length coordinate for each spline shown in Fig. 4. More definite conclusions can be drawn from it. First, note that CBS is indeed capable of giving the ideal circle. The wavy character of the graph is a reflection of an insufficient number of imaginary points — the more points, the smoother the curvature. Second, Bezier splines give noticeable deviation from the ideal circle for all parameters of optimization (distances from endpoints). Third, GNB is a very powerful technique, which depends on the chosen length of the beam. In case, when the prescribed length of GNB coincides with the length of the ideal circle, it actually gives this ideal circle.

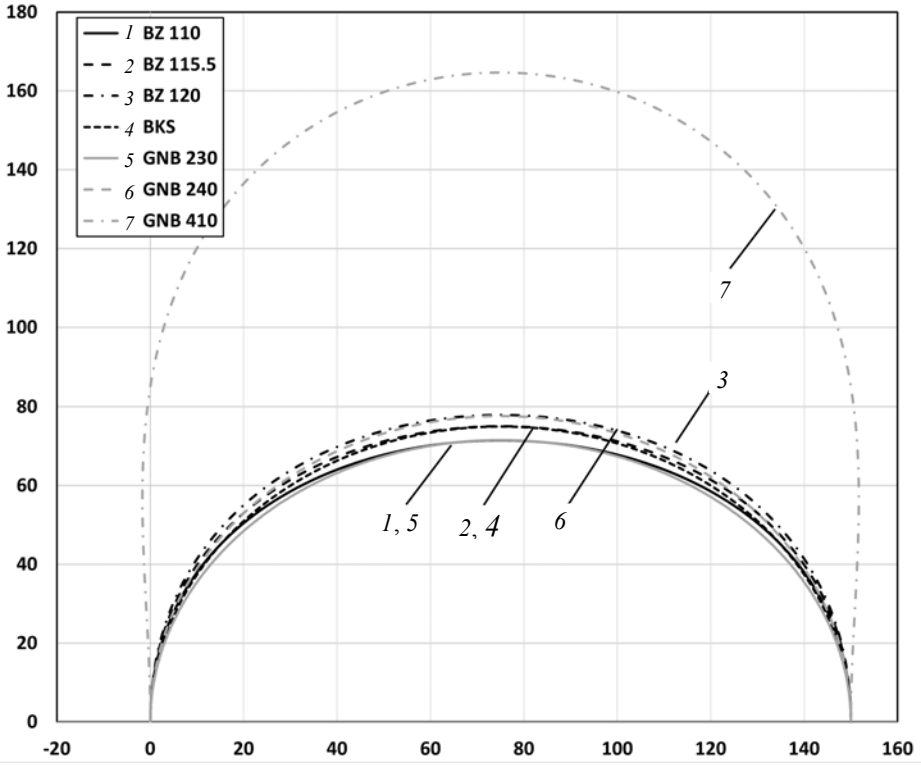

Fig. 3. Several calculated splines according to the Bezier method (4 points), BCS, and GNB

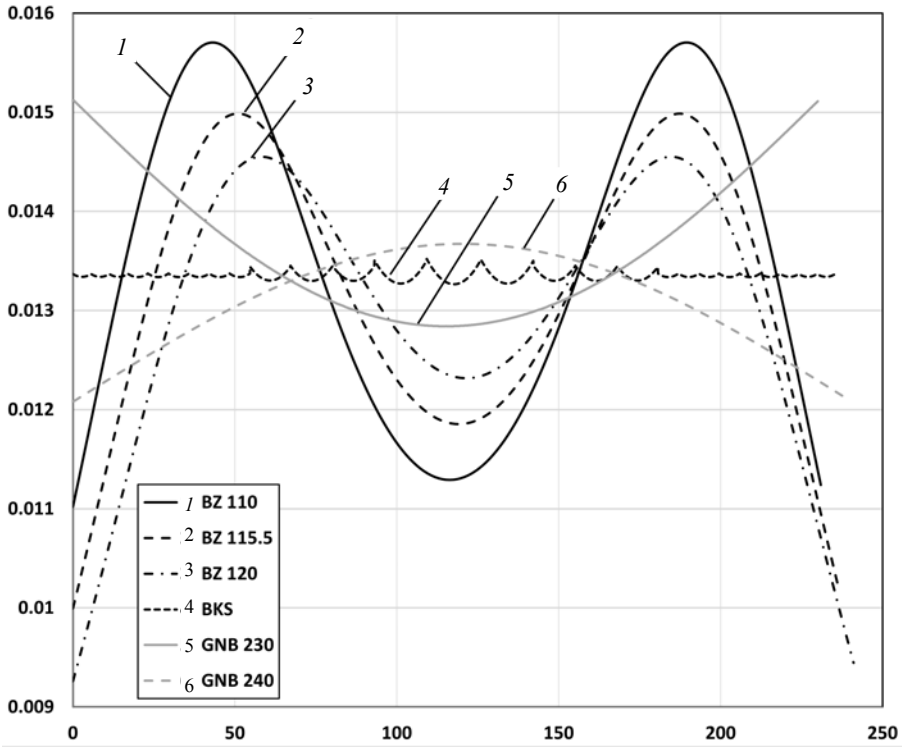

Fig. 4. The graphs of curvatures obtained by different splines for Task 1

Compare the quality (energy) of each depicted curve. The results of its calculation are given in Table 1, where the absolute value of energy, as well as the reduced value of it (divided by the ideal semi-circle value of 0.41888), are presented. The result for CBS is slightly different from the ideal circle due to a smaller number of imaginary points (only 28 points are employed here). As to Bezier's results, they are close to 1 in the considered range of chosen distances of additional points, and the lowest result is attained for the BZ 120 curve.

Table 1. Calculated energies for different splines for Task 1

Curve	BZ 110	BZ 115.5	BZ 120	BCS	GNB 230	GNB 240	GNB 410
Quality	0.04305	0.04190	0.04113	0.04190	0.043024	0.041181	0.037927
Reduced quality	1.02774	1.0003	0.9818	1.0003	1.04475	0.98312	0.90544

Evidently, the notion of energy cannot be the sole criterion of fairness. Note, that splines, which "embrace" the ideal semi-circle give the lesser values of energy. Concerning the results of Table 1 it is interesting to recall the results of Horn [42]. Remind that for this task 1 the "best" value of energy equal to 0.91383 was obtained [42]. So, plot the graph of the energy concerning beam length by GNB approach, Fig. 5. Interesting to note, that in the vicinity of the ideal semi-circle configuration ($L = L_0 = 235.6$) the quality of the curve linearly decreases with length. Yet in the range of length $310 < L < 340$, it attends the local "plateau". The calculated quality in this range is approximately equal to 0.03828 (at $L = 320$). Dividing this value by 0.041888 (ideal semi-circle) we get the reduced value equal to 0.9138, which is very close to Horn's theoretical value. This testifies to the high efficiency of the GNB approach [2]. Further increase of L beyond this range leads to a permanent slow decrease of energy, which was not predicted in Horn analysis [42]. This is related to the outward deviation of the calculated figure from the vertical lines $x = 0$ and $x = 150$, which is evident from Fig. 3 for GNB 410. For $L \to \infty$ the energy tends to zero.

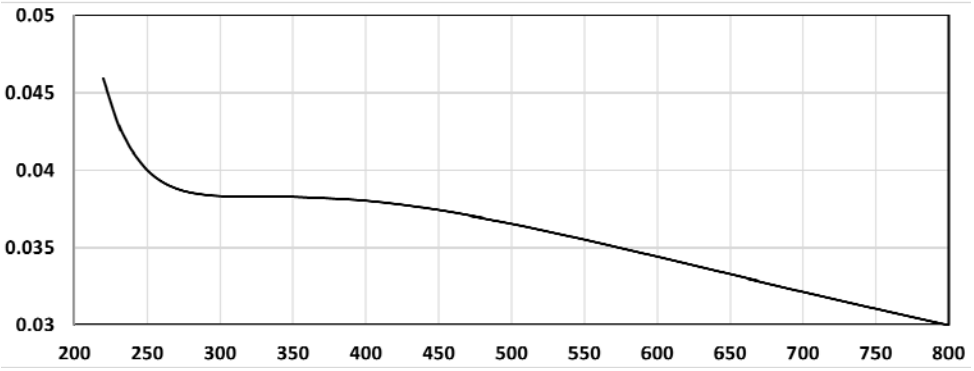

Fig. 5. Quality of GNB spline concerning the beam length for Task 1

Example task 2

This task is very similar to symmetrical Task 1. The only difference is that in first point B_1 the tangent angle is inclined to $-60°$ concerning the horizontal axis, and in second point B_2 the angle is equal to $60°$.

Intuitively, the best expected (ideal) curve is the semi-circle. From geometrical consideration, its diameter should satisfy the following relation $D/2\cos 30° = 75$, where one can get that $D = 173.20$. So, the length of the ideal figure is equal to 181.37. As to energy (1) of the ideal curve, it is equal to 0.02418.

Construct the splines according to different techniques, Fig. 6. As above CBS gives the ideal semi-circle. Bezier spline gives very close results at a distance equal to 67. When this distance is smaller, than Bezier curve lies below the ideal circle, and when the distance is larger it is situated above the ideal curve. A similar picture is for GNB splines. When their lengths are lesser than the ideal circle length, it is placed below, and above otherwise.

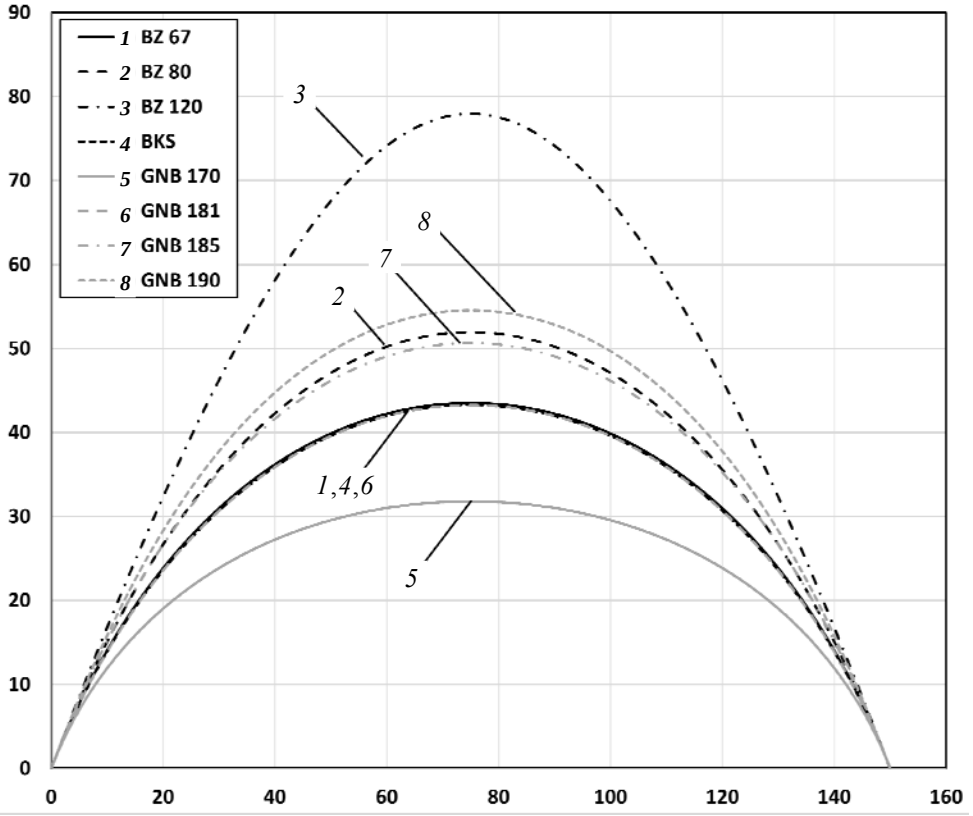

Fig. 6. Several calculated splines according to the Bezier method, BCS, and GNB, Task 2

The informative is a graph of curvatures for each spline, shown in Fig. 7. The best Bezier spline, BZ 67, is very close to the ideal circle, and its curvature is almost ideal. The same can be said about the BCS and GNB 185. Compared with CBS for Task 1 (Fig. 4), the curvature for CBS for Task 2 is much smoother: we use here as many as 120 imaginary points. Graphs of curvature are very important to judgment about the quality of different splines.

Compare the quality (energy) of each depicted curve. The results of its calculation for Task 2 are given in Table 2. That results in differently-looking curves that sometimes are very close. This means, that energy cannot be the sole criterion of the construction of the curve nor for the assessment of its fairness.

T a b l e 2 . Calculated energies for different splines for Task 2

Curve	BZ 67	BZ 80	BZ 120	BCS 181	GNB 170	GNB 181	GNB 190
Quality	0.0241	0.0246	0.0408	0.0242	0.0303	0.0242	0.0243

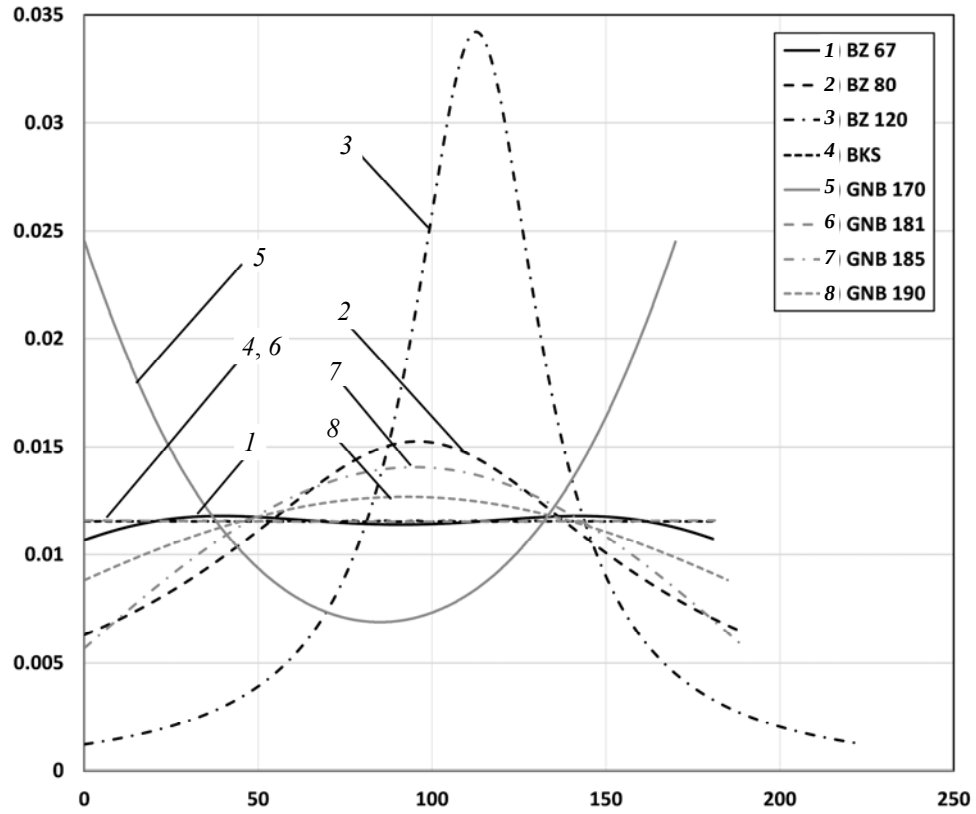

Fig. 7. The graphs of curvatures obtained by different splines for Task 2

Example task 3

This task is a more complicated one and relates to the construction of anti-symmetrical geometry. Point B_1 has coordinates $(X=0,\ Y=0)$, second point B_2 has coordinates $(X=150, Y=150)$, the tangent in point B_1 is directed at an angle *of* $60°$, while in point B_2 the angle is equal to $60°$, too.

The best solution cannot be formulated intuitively, so here we will subjectively assess the best solution below.

Construct the splines according to different techniques, Fig. 8. Look on the CBS, which does not require any auxiliary parameters. The general subjective impression is that it is visually pleasant, and its calculated length is about 294. So, chose the auxiliary parameters in other spline methods to approach this spline. It is not always possible for the Bezier splines. If we take the distance to be very small – it would resemble the straight line between two endpoints, and, of course, it should be rejected. If we take the distance in the Bezier spline too large, the graph will be placed well beyond the vertical range of $-150 < y < 150$. So, we chose subjectively the distances equal to 120, 150, and 180 as the candidates for

the best Bezier curve. Nevertheless, they are not pleasantly looking, and this can be supported by graphs of curvatures, Fig. 9. As to GNB it completely coincides with CBS, if we take its length as large as 294, Fig. 8. The increase or decrease of length leads to more loose or tight geometry, respectively.

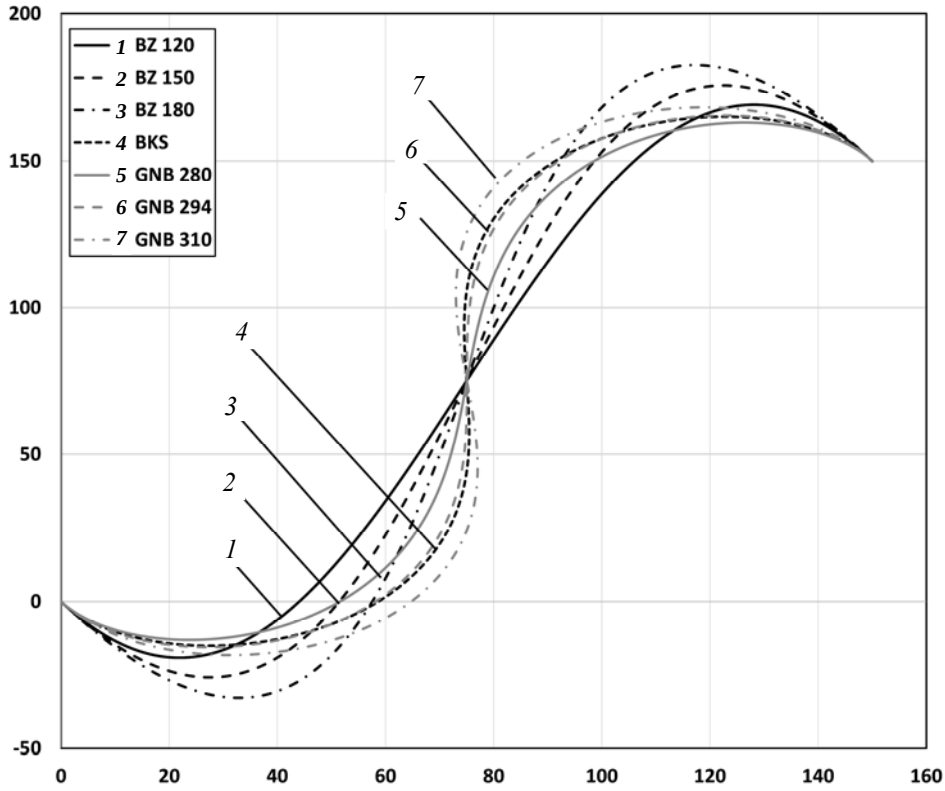

Fig. 8. Several calculated splines according to the Bezier method, BCS, and GNB, Task 3

More informative are the graphs of curvatures concerning the current length coordinate, Fig. 9. The curvature of CBS is very smooth, it is a straight line (small fluctuations are due to a limited number of imaginary points). So, an important conclusion can be drawn from its visual presentation. The CBS is a Cornu spiral, and this can be explained by the third differential equation of (6). On each small straight section $P = \text{const}$, so the moments (curvature) change linearly. In case, if intermediate points are the imaginary ones, the force does not change between them, so the whole section between any real points is a Cornu spiral.

As one can see, the GNB completely coincides with the CBS, in case its length is equal to the length of CBS. If GNB is shorter than CBS, then its curvature is larger than that of CBS. And vice versa, for longer GNB its curvature is smaller. As to the Bezier curve, it demonstrates the large local curvatures for all three considered distances chosen. As we see, the Bezier curve is ineffective for anti-symmetric cases.

Compare the energy for each curve. The results of its calculation for Task 3 are given in Table 3. The results for Bezier curves are very poor. So, the very big difference in energy can testify to the deficiency of the curve. As to GNB, the results for it are close to CBS because their lengths are similar. In any case, by varying the length of GNB the quality of it can always be better than that of CBS.

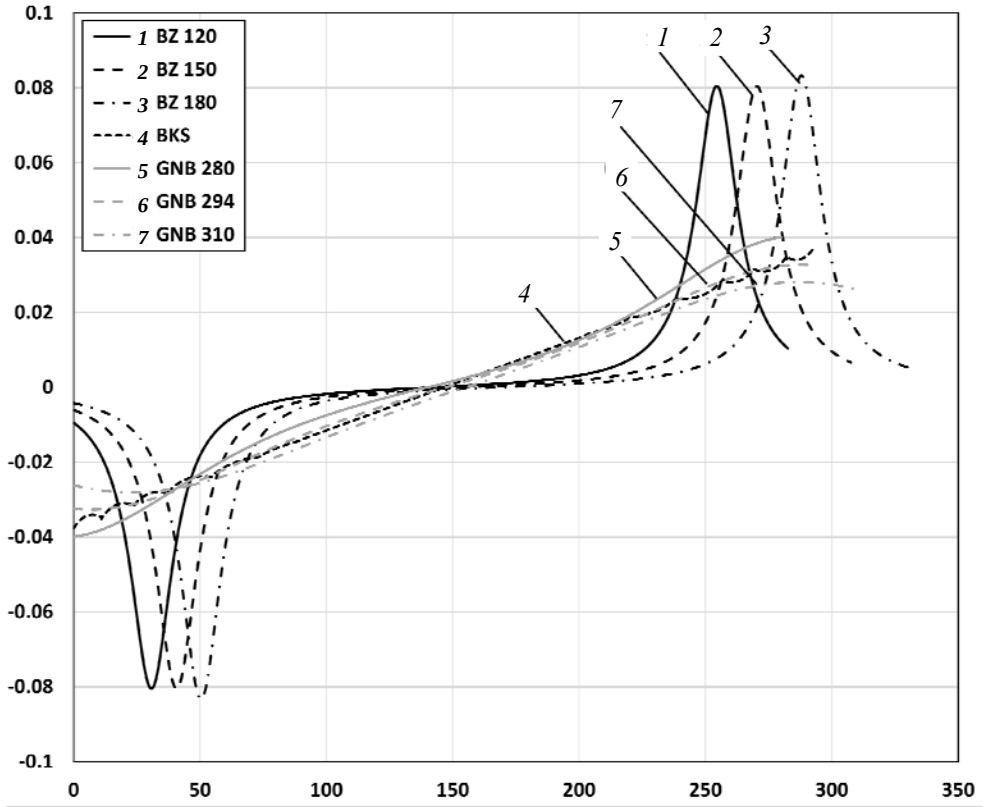

Fig. 9. The graphs of curvatures obtained by different splines for Task 3

Table 3. Calculated energies for different splines for Task 3

Curve	BZ 120	BZ 150	BZ 180	BCS	GNB 280	GNB 294	GNB 310
Quality	0.2080	0.2092	0.2173	0.1286	0.1373	0.1284	0.1225

Example task 4

This task is similar to the previous one but is not an antisymmetric. Point B_1 has coordinates $(X = 0, Y = 0)$, second point B_2 has coordinates $((X = 150,$ $Y = -150)$, the tangent in point B_1 is directed at an angle — $60°$, while in point B_2 the angle is equal to $0°$.

The best solution cannot be formulated intuitively, so here we will subjectively assess the best solution below.

Construct the splines according to different techniques, Fig. 10. As to CBS, the general subjective impression is that it is visually pleasant, and its calculated length is about 260. So, chose the auxiliary parameters in other splines as to approach this spline. As in Task 3, it is not possible for the Bezier splines – they deflect from CBS for any chosen parameter of distance. So, the results for Bezier splines are shown for three subjectively chosen distances – 100, 125, and 150. Nevertheless, they are not pleasantly looking, and this impression can be

supported by graphs of curvatures, Fig. 11, which has large local peaks of curvature, which is prohibited for "fair" spline [12]. As to GNB it completely coincides with CBS if we take its length as 260, Fig. 10. The increase or decrease of length leads to more loose or tight geometry, respectively.

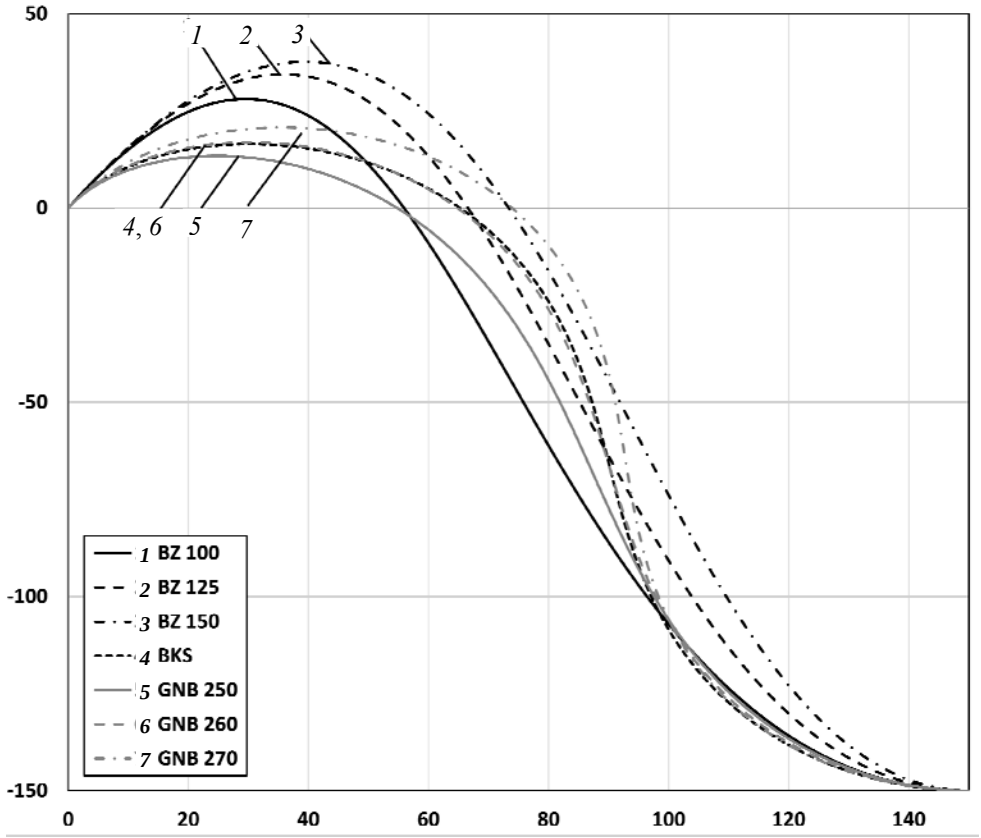

Fig. 10. Several calculated splines according to the Bezier method, BCS, and GNB, Task 4

Informative are the graphs of curvatures concerning the current length coordinate, Fig. 11. The curvature of CBS is a straight line (small fluctuations are due to a limited number of imaginary points), so evidently CBS is a Cornu spiral.

As in above Task 3, note that GNB completely coincides with CBS in case, its length is equal to the length of CBS and can be more tight or loose depending on whether the length of GNB is shorter or longer than the length of CBS. Bezier curve demonstrates the large curvatures for all three distances chosen.

Compare the energy for each curve. The results of its calculation for Task 4 are given in Table 4. The results for Bezier curves are very poor and testify to the deficiency of the curve. As to GNB, the results for energy are close for CBS because their lengths are similar. In any case, by varying the length of GNB the quality of it can always be better than that of CBS.

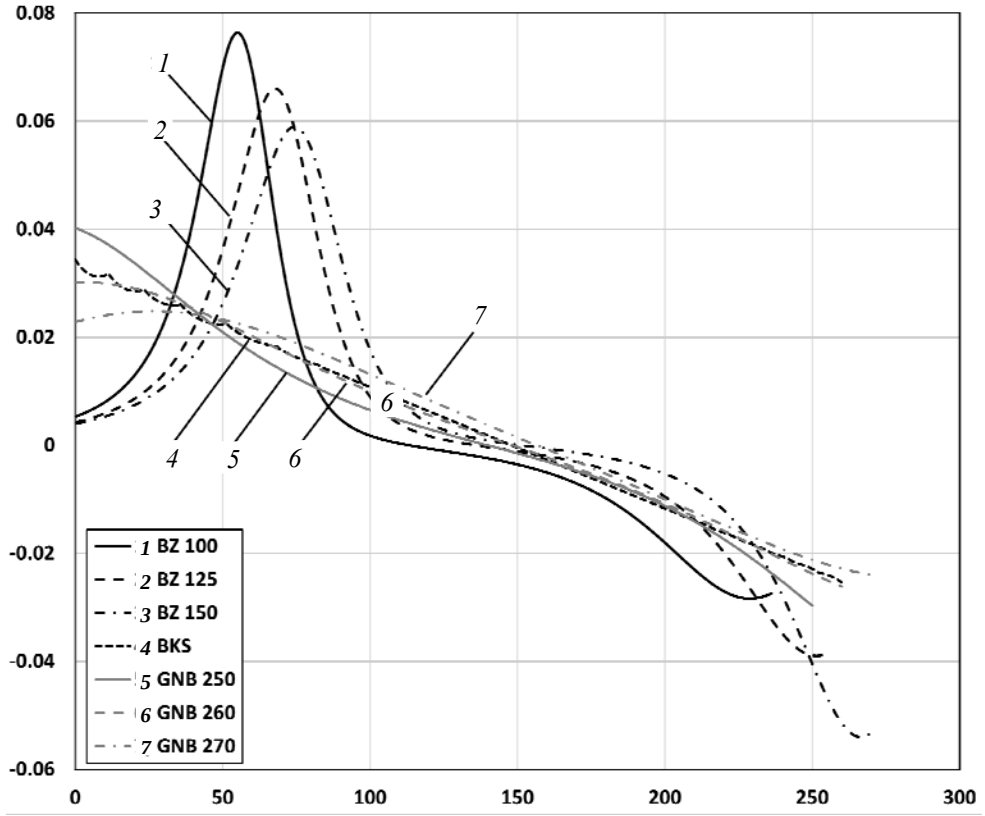

Fig. 11. The graphs of curvatures obtained by different splines for Task 4

Table 4. Calculated energies for different splines for Task 4

Curve	BZ 100	BZ 125	BZ 150	BCS	GNB 250	GNB 260	GNB 270
Quality	0.1156	0.1114	0.1153	0.0781	0.0835	0.0778	0.0753

CONCLUSION

The main attention of the paper is paid to the discussion of the advantages of CBS. On one hand, it is the four degrees of freedom simplified version of GNB, which operates by 6 degrees of freedom at each point. The beam theory origin of CBS gives a wide prospect for its modernization and application. On the other hand, the presented here version of CBS for the task of interpolation is reduced to the new original technique of construction of the Cornu spiral, which is widely recognized as one of the most aesthetic curves for the geometrical design purpose [62]. The application of the methodology of linear TMM makes this technique very simple and effective.

In detail, the method and its comparison with Brazier spline and GNB is made on the example of two endpoints that are connected by spline with prescribed tangent values. Several local conclusions can be drawn out.

1. As to the Brazier spline with the employment of four points (two intermediate ones can be chosen arbitrarily to optimize the geometry), it generally demonstrates poorer results. The resulting curvatures, especially for geometries, when

it changes the sign, behave very unsmoothly and exhibit very high local peaks. In this case, the calculated value of energy (1) is much higher than for CBS.

2. CBS for all 4 tasks considered gives very pleasant results. In all cases, the curvature is either constant (symmetric cases) or linearly changes with the spline length coordinate. The only technical requirement for its realization is the insertion of a sufficient number of imaginary points.

3. GNB is the most effective technique for spline construction as well as for modeling the deformation of real flexible beams. Its drawback for the geometrical design is that the justified length of the beam should be chosen in advance. The value obtained by the CBS solution is a good initial approximation for further GNB application. The accuracy of the GNB technique is demonstrated in the example of the well-known Horn task [42].

4. Energy criteria of fairness (1) cannot be considered as a sole criterion for the spline construction. On the other hand, a very big value of it testifies to the drawback of the applied technique.

REFERENCES

1. I. Orynyak, D. Koltsov, O. Chertov, and R. Mazuryk, "Application of beam theory for the construction of twice differentiable closed contours based on discrete noisy points," *System Research and Information Technologies*, no. 4, pp. 119–140, 2022. doi: https://doi.org/10.20535/SRIT.2308-8893.2022.4.10
2. I. Orynyak, R. Mazuryk, and A. Oryniak, "Basic (discontinuous) and smoothing up (conjugated) solutions in transfer matrix method for static geometrically nonlinear beam and cable in plane," *Journal of Engineering Mechanics*, vol. 146, no. 5, 2020. doi: https://doi.org/10.1061/(ASCE)EM.1943-7889.0001753
3. J.H. Alberg, E.N. Nilson, and J.L. Walsh, *The theory of splines and their applications*. New York: Academic, 1967.
4. G. Farin, "History of Curves and Surfaces in CAGD," *Handbook of CAGD*, G. Farin, M.S. Kim, and J. Hoschek (Eds), 2002. doi: https://doi.org/10.1016/B978-044451104-1/50002-2
5. J.C. Holladay, "A smoothest curve approximation," *Math. Tables Aids Comput*., 11, pp. 233–243, 1957. doi: https://doi.org/10.2307/2001941
6. R.H. Bartels, J.C. Beatty, and B.A. Barsky, *An introduction to splines for use in computer graphics and geometric modeling*. Morgan Kaufmann, 1995.
7. Daniel G. Schweikert, "An Interpolation Curve using a Spline in Tension," *Journal of Mathematics and Physics*, 45, pp. 312–317, 1966. doi: https://doi.org/10.1002/sapm1966451312
8. S.P. Timoshenko, *Strength of Materials: Part II Advanced Theory and Problems*. D. Van Nostrand, 1956.
9. Even Mehlum, "A Curve-Fitting Method Based on a Variational Criterion," *BIT*, 4, pp. 213–223, 1964.
10. P.H. Wagner, X. Luo, and K.A. Stelson, "Smoothing curvature and torsion with spring splines," *Computer-Aided Design*, 27, pp. 615–626, 1995. doi: https://doi.org/10.1016/0010-4485(95)99798-d
11. Asker Bengt, "The Spline Curve, A Smooth Interpolating Function Used in Numerical Design of Ship-Lines," *BIT*, 2, pp. 76–82, 1962.
12. H.P. Moreton, "Minimum curvature variation curves, networks, and surfaces for fair free-form shape design," Doctoral dissertation, University of California, Berkeley, 1992.
13. K. Salkauskas, "C1 Splines for Interpolation of Rapidly Varying Data," *Rocky Mountain Journal of Mathematics*, 14, pp. 239–250, 1984.
14. G. Birkhoff, H. Burchard, and D. Thomas, *Nonlinear Interpolation by Splines, Pseudosplines, and Elastica*. General Motors Research Laboratories Report 468, 1965.

15. D.F. Rogers, *An introduction to NURBS: with historical perspective*. Morgan Kaufmann, 2001.
16. James Ferguson, "Multivariable Curve Interpolation," *Journal of the Association of Computing Machinery*, 11, pp. 221–228, 1964.
17. M.P. Epstein, "On the influence of parametrization in parametric interpolation," *SIAM Journal on Numerical Analysis*, 13(2), pp. 261–268, 1976.
18. J.A. Kjellander, "Smoothing of cubic parametric splines," *Computer-Aided Design*, 15(3), pp. 175–179, 1983.
19. J. Ye, R. Qu, "Fairing of parametric cubic splines," *Mathematical and Computer Modelling*, 30(5-6), pp. 121–131, 1999. doi: https://doi.org/10.1016/S0895-7177(99)00152-1
20. A. Binninger, O. Sorkine-Hornung, "Smooth Interpolating Curves with Local Control and Monotone Alternating Curvature," in *Computer Graphics Forum*, vol. 41, no. 5, pp. 25–38, 2022. doi: https://doi.org/10.1111/cgf.14600
21. R. Levien, C.H. Séquin, "Interpolating splines: Which is the fairest of them all?" *Computer-Aided Design and Applications*, 6(1), pp. 91–102, 2009. doi: https://doi.org/10.3722/cadaps.2009.91-102
22. G. Brunnett, J. Kiefer, "Interpolation with minimal-energy splines," *Computer-Aided Design*, 26(2), pp. 137–144, 1994. doi: https://doi.org/10.1016/0010-4485(94)90034-5
23. R.C. Veltkamp, W. Wesselink, "Modeling 3D curves of minimal energy," in *Computer Graphics Forum*, vol. 14, no. 3, pp. 97–110. Edinburgh, UK: Blackwell Science Ltd., 1995. doi: https://doi.org/10.1111/j.1467-8659.1995.cgf143_0097.x
24. L. Fang, D.C. Gossard, "Multidimensional curve fitting to unorganized data points by nonlinear minimization," *Computer-Aided Design*, 27(1), pp. 48–58, 1995. doi: https://doi.org/10.1016/0010-4485(95)90752-2
25. G. Birkhoff, C.R. de Boor. "Piecewise Polynomial Interpolation and Approximation," in *Approximation of Functions*, ed. H.L. Garabedian, pp. 164–190. Elsevier, New York/Amsterdam, 1965.
26. G. Farin, G. Rein, N.S. Sapidis, and A.J. Worsey, "Fairing Cubic B-Spline Curves," *Computer Aided Geometric Design*, pp. 91–103, 1987. doi: https://doi.org/10.1016/0167-8396(87)90027-6
27. Alfred M. Bruckstein, Robert J. Holt, and Arun N. Netravali, "Discrete elastica," *Applicable Analysis*, 78, 3-4, pp. 453–485, 2001. doi: https://doi.org/10.1080/00036810108840945
28. G. Xu, G. Wang, and W. Chen, "Geometric construction of energy-minimizing Béezier curves," *Science China Information Sciences*, 54, pp. 1395–1406, 2011. doi: https://doi.org/10.1007/s11432-011-4294-8
29. D. Brander, J.A. Bærentzen, A.S. Fisker, and J. Gravesen, "Bézier curves that are close to elastic," *Computer-Aided Design*, 104, pp. 36–44, 2018. doi: https://doi.org/10.1016/j.cad.2018.05.003
30. C. Zhang, P. Zhang, and F.F. Cheng, "Fairing spline curves and surfaces by minimizing energy," *Computer-Aided Design*, 33(13), pp. 913–923, 2001. doi: https://doi.org/10.1016/S0010-4485(00)00114-7
31. D.B. Parkinson, D.N. Moreton, "Optimal biarc-curve fitting," *Computer-Aided Design*, 23(6), pp. 411–419, 1991. doi: https://doi.org/10.1016/0010-4485(91)90009-L
32. G. Xu, Y. Zhu, L. Deng, G. Wang, B. Li, and K.C. Hui, "Efficient construction of B-spline curves with minimal internal energy," *Computers, Materials & Continua*, 58(3), pp. 879–892, 2019. doi: https://doi.org/10.32604/cmc.2019.03752
33. J. Li, "Combined internal energy minimizing planar cubic Hermite curve," *Journal of Advanced Mechanical Design, Systems, and Manufacturing*, 14(7), 2020.
34. R. Levien, *The elastica: a mathematical history*. Electrical Engineering and Computer Sciences University of California at Berkeley, Technical Report No. UCB/EECS-2008-103, 2008.
35. Garrett Birkhoff, Carl R. de Boor, "Piecewise polynomial interpolation and approximation," *Proc. General Motors Symp. of 1964*, pp. 164–190.
36. E.H. Lee, G.E. Forsythe, "Variational study of nonlinear spline curves," *SIAM review*, 15(1), pp. 120–133, 1973. doi: https://doi.org/10.1137/1015004

37. G.H. Brunnett, "Properties of minimal-energy splines," in *Curve and surface design*; Society for Industrial and Applied Mathematics, pp. 3–22, 1992. doi: https://doi.org/10.1137/1.9781611971651.ch1
38. J.M. Glass, "Smooth-curve interpolation: A generalized spline-fit procedure," *BIT Numerical Mathematics*, 6(4), pp. 277–293, 1966. doi: https: //doi.org/10.1007/BF01966089
39. M.A. Malcolm, "On the computation of nonlinear spline functions," *SIAM Journal on Numerical Analysis*, 14(2), pp. 254–282, 1977. doi: https://doi.org/10.1137/0714017
40. Even Mehlum, *Curve and Surface Fitting Based on Variational Criteria for Smoothness*. Central Institute for Industrial Research, Oslo, Norway, 1969.
41. E. Cohen, T.Lyche, and R.F. Riesenfeld, "MCAD: Key historical developments,' *Computer methods in applied mechanics and engineering*, 199(5-8), pp. 224–228, 2010. doi: https://doi.org/10.1016/j.cma.2009.08.003
42. B.K. Horn, "The curve of least energy," *ACM Transactions on Mathematical Software (TOMS)*, 9(4), pp. 441–460, 1983. doi: https://doi.org/10.1145/356056.356061
43. M. Kallay, "Plane curves of minimal energy," *ACM Transactions on Mathematical Software (TOMS)*, 12(3), pp. 219–222, 1986. doi: https://doi.org/10.1145/7921.7924
44. M. Kallay, "Method to approximate the space curve of least energy and prescribed length," *Computer-Aided Design*, 19(2), pp. 73–76, 1987. doi: https://doi.org/ 10.1016/S0010-4485(87)80048-9
45. D. Brander, J. Gravesen, and T.B. Nørbjerg, "Approximation by planar elastic curves," *Adv. Comput. Math.*, 43, pp. 25–43, 2017. doi: https://doi.org/10.1007/ s10444-016-9474-z
46. O.M. O'Reilly, *Modeling nonlinear problems in the mechanics of strings and rods*, pp. 187–268. Cham: Springer International Publishing, 2017. doi: https://doi.org/10.1007/978-3-319-50598-5
47. C. Meier, A. Popp, and W.A. Wall, "Geometrically exact finite element formulations for slender beams: Kirchhoff–Love theory versus Simo–Reissner theory," *Archives of Computational Methods in Engineering*, 26(1), pp. 163–243, 2019. doi: https://doi.org/10.1007/s11831-017-9232-5
48. Y. Goto, Y. Morikawa, and S. Matsuura, "Direct Lagrangian nonlinear analysis of elastic space rods using transfer matrix technique," *Proc. of JSCE, Struct. Eng./Earthquke Eng.*, 5(1), 1986.
49. A. Rosen, O. Gur, "A transfer matrix model of large deformations of curved rods," *Computers & Structures*, 87(7-8), pp. 467–484, 2009. doi: https://doi.org/10.1016/ j.compstruc.2008.12.014
50. I.V. Orynyak, S.A. Radchenko, "A mixed-approach analysis of deformations in pipe bends. Part 3. Calculation of bend axis displacements by the method of initial parameters," *Strength of materials*, 36, pp. 463–472, 2004. doi: https://doi.org/10.1023/B:STOM.0000048394.98411.4f
51. F. Leckie, E. Pestel, "Transfer-matrix fundamentals," *International Journal of Mechanical Sciences*, 2(3), pp. 137–167, 1960. doi: https://doi.org/10.1016/0020-7403(60)90001-1
52. J.H. Argyris et al., "Finite element method—the natural approach," *Computer Methods in Applied Mechanics and Engineering*, 17, pp. 1–106, 1979. doi: https://doi.org/10.1016/0045-7825(79)90083-5
53. M.A. Crisfield, "A consistent co-rotational formulation for non-linear, three-dimensional, beam-elements," *Comput. Methods Appl. Mech. Eng.*, 81, pp. 131–150, 1990. doi: https://doi.org/10.1016/0045-7825(90)90106-V
54. A.H. Fowler, C.W. Wilson, *Cubic Spline, a Curve Fitting Routine*, Report No. Y-1400, Contract No. W-7405-ENG-26, Nuclear Division, Union Carbide Corp., Oak Ridge, Tenn., 1962, pp. 1–41.
55. W.D. Birchler, S.A. Schilling, *Comparisons of Wilson–Fowler and Parametric Cubic Splines with the Curve-Fitting Algorithms of Several Computer-Aided Design Systems (No. LA-13784)*. Los Alamos National Lab. (LANL), Los Alamos, NM (United States), 2001. https://doi.org/10.2172/776180
56. I.V. Orynyak, I.V. Lokhman, and A.V. Bogdan, "Determination of curve characteristics by its discrete points measured with an error and its application to stress analysis

for buried pipeline," *Strength of Materials*, 44, pp. 268–284, 2012. doi: https://doi.org/10.1007/s11223-012-9380-7

57. I.V. Orynyak, A.V. Bohdan, and I.V. Lokhman, "The 2d Spring Splines procedure application with prescribed accuracy for determination of the global (pipe centerline) as well as the local (dent) curvatures," *International Pipeline Conference*, 12, pp.171–181, 2012. doi: https://doi.org/10.1115/ipc2012-90127
58. A. Borum, T. Bretl, "The free configuration space of a Kirchhoff elastic rod is path-connected," in *2015 IEEE International Conference on Robotics and Automation (ICRA)*, pp. 2958–2964. doi: https://doi.org/10.1109/ICRA.2015.7139604
59. David Brander et al., "Designing for hot-blade cutting: Geometric Approaches for High-Speed Manufacturing of Doubly Curved Architectural Surfaces," in *Advances in Architectural Geometry 2016*, pp. 306–327. doi: https://doi.org/10.3218/3778-4_21
60. S.P. Timoshenko, *Strength of materials: Part 1: Elementary theory and problems*. N.-Y.: Robert E. Krieger, 1958.
61. I. Orynyak, R. Mazuryk, "Application of method of discontinuous basic and enhanced smoothing solutions for 3D multibranched cable," *Engineering Structures*, 251, 113582, 2022. doi: https://doi.org/10.1016/j.engstruct.2021.113582
62. K.T. Miura, G. Ru, "Aesthetic curves and surfaces in computer-aided geometric design," *International Journal of Automation Technology*, 8(3), pp. 304–316, 2014. doi: https://doi.org/10.20965/ijat.2014.p0304

Received 26.04.2024

INFORMATION ON THE ARTICLE

Igor V. Orynyak, ORCID: 0000-0003-4529-0235, National Technical University of Ukraine "Igor Sikorsky Kyiv Polytechnic Institute", Ukraine, e-mail: igor_orinyak@yahoo.com

Petro M. Yablonskyi, ORCID: 0000-0002-1971-5140, National Technical University of Ukraine "Igor Sikorsky Kyiv Polytechnic Institute", Ukraine, e-mail: ypn@ukr.net

Dmytro R. Koltsov, ORCID: 0000-0002-0396-7255, National Technical University of Ukraine "Igor Sikorsky Kyiv Polytechnic Institute", Ukraine, e-mail: koltsovdd@gmail.com

Oleg R. Chertov, ORCID: 0000-0003-0087-1028, National Technical University of Ukraine "Igor Sikorsky Kyiv Polytechnic Institute", Ukraine, e-mail: chertov@i.ua

Roman V. Mazuryk, ORCID: 0000-0003-4309-824X, National Technical University of Ukraine "Igor Sikorsky Kyiv Polytechnic Institute", Ukraine, e-mail: r.mazuryk.ua@gmail.com

ДОБРОТНІСТЬ 2D КОРОТАЦІЙНОГО СПЛАЙНУ ПРОМЕНЯ ПОРІВНЯНО З ГЕОМЕТРИЧНО НЕЛІНІЙНО ПРУЖНИМ ПРОМЕНЕМ / І.В. Ориняк, П.М. Яблонський, Д.Р. Кольцов, О.Р. Чертов, Р.В. Мазурик

Анотація. Метою статті є подальше дослідження властивостей і переваг нещодавно запропонованого коротаційного балкового сплайну (КБС). Акцент зроблено на розгляді досить простої задачі проведення сплайну між двома кінцевими точками із заданими дотичними в них. Як критерій «хорошості» сплайну обрано відоме поняття «добротності», яке являє собою інтеграл від квадрата кривини сплайну по його довжині, що походить із теорії пружної балки як енергія деформації. Порівняння «добротності» КБС виконано з деякими варіантами кубічної кривої Безьє (КБ) і геометрично нелінійної балки (ГНБ) зі змінною довжиною. Показано, що КБС є набагато ефективнішим, ніж КБ, для якої будь-яка спроба забезпечити кращу «добротність» КБ шляхом зміни відстані від кінцевих точок до двох проміжних точок, як правило, призводить до гірших результатів порівняно з КБС. З іншого боку, ГНБ, або іншими словами, крива «еластика», здатна давати дещо кращі значення «добротності» для оптимальної довжини балки. Це можна пояснити більш складною методологічною основою ГНБ, яка використовує 6 ступенів вільності в кожному перерізі порівняно з 4-ма ступенями вільності в КБС.

Ключові слова: коротаційний балковий сплайн, геометрично нелінійна балка, плоска задача, крива Безьє, добротність, метод початкових параметрів.